



# THE ERA OF FORCED RESONANT SOFT-SWITCHING

White Paper

## ABSTRACT

The power electronics market is always in pursuit of power converter efficiencies and lowering costs. The approach has been to reliably and economically reduce switching and conduction losses; most recently by employing ever more innovative topologies and semiconductor materials, like the newest generation of silicon IGBTs and MOSFET trench designs and faster SiC and GaN MOSFETs. Bringing switching times down, however, results in intolerable levels of  $dV/dt$  and EMI. Pre-Switch introduces a new, third option based on forced resonance soft-switching driven by Artificial Intelligence (AI). The Pre-Switch AI is resident on a new IC controller, which works across all transistor types, load ranges and over a wide input voltage range. This revolutionary, low-cost technology enables a 70-95% reduction in switching losses and solves the  $dV/dt$  problems associated faster transistors.

**Alberto Guerra**

Pre-Switch, Technical Advisor

# Introduction

The Power electronics market is experiencing an unprecedented growth phase punctuated with renaissance-like innovation. Power electronics applications have been deployed in more places than ever before, and the application space continues to expand. New materials, innovative packaging, and advanced digital control techniques help engineers and device manufacturers in the pursuit of improving conversion efficiency, reducing power losses, reducing weight, and bringing down cost. These issues are all on the critical path to unlocking the next wave of human innovation.

Power electronics have made a significant contribution to shaping the world as we know it today. Nearly 60 percent of all electric energy produced worldwide is used to power motors of all sizes, shapes, and efficiencies. Variable speed drives have helped—and continue to help—save as much as 70 percent of energy costs by their ability to control motor speed based on load. Emerging energy efficiency standards naturally force the adoption of electronically-controlled motors; however, these present many challenges to electronics designers determined to offer ever more efficient systems.

In Europe, of example, the Energy-Related Products Directive (ErP), has had a dramatic impact on the efficiency of motors with electric input power up to 500KW since its ratification in January 2013. A similar directive (641/2009) covers motors used in recirculation pumps and other industrial applications. The full impact of these standards will be in force by 2020 and represents 34 terawatt-hours of electrical

energy savings by 2020; the equivalent of removing 16 Million tons of CO<sub>2</sub> emission annually.

Emerging domains like Industry 4.0 and Industrial Internet of Things (IIoT) are also pushing industry suppliers towards smarter and more efficient motors and motor controls. More than 51 million industrial motor drives (Figure 1) and 200 million industrial motors (Figure 2) are produced each year. The opportunity for growth is massive. However, the traditional single-digit percentage point improvements in efficiency in electric motor drives is simply not sufficient to meet these markets and their governing standards. Ambitious government regulations require ambitious new designs for energy efficient solutions in appliances, data centers, heating and ventilation systems, water circulation and pumping systems, PV solar inverters, and so on. It is an undisputable fact that these advances must all come at market-sustaining economics.



Figure 1: Industrial Motors and Industrial Motor Drives annual production.



Figure 2: Global electric motor shipments.

The advances the power industry has made to-date would not have been possible without continuous improvement of semiconductor technology as well as a laser-like focus on improving efficiency and reducing cost.

**Opportunity: PV Solar**

According to the latest *Global Solar Demand Monitor* published by *GTM Research*, the annual installations of solar capacity are expected to rise by 6% to ~104 GW in 2018 [8]. Annual installations will remain above 100 GW through at least 2022, according to the report. It is clear how the growth in power generation from solar photovoltaics, has remained almost constant for over 25 years (Figure 3). All that power must be processed, controlled and distributed, and re-converted by power electronics and power semiconductors.

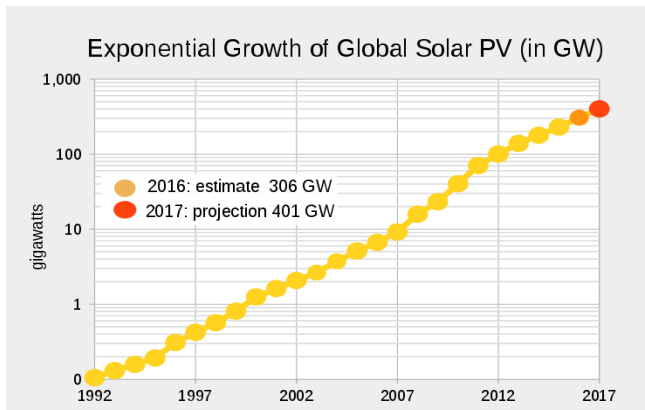


Figure 3: Total installed solar PV power, worldwide

**Opportunity: Energy storage and the electric vehicle (EV) revolution**

The dramatic reduction in cost of Li-Ion batteries has opened a vast new market for power electronics, the least of which are not grid-connected storage systems, as well as the

seemingly unstoppable electro-mobility revolution led by the automotive industry. Annual grid-connected battery installations grew by 53 percent in 2017 to 1.9 GW, the highest level on record. More than 3 GW of battery storage is forecasted to be deployed in 2018, and global project pipeline projections from the end of the first quarter of 2018, show the storage project pipeline at a staggering 10.4 GW. [10] [11]

This growth, however, pales in comparison to what the full impact on this segment will be in the next 12-15 years, especially when one considers the exponential growth of electric cars and trucks. A recent study published by McKinsey forecast for the annual Li-ion battery demand to reach 2900 GWh by 2030. Again, the vast majority of this demand is projected to be in the automotive (~60 percent) and utility scale and distributed storage (~30 percent) segments, while the consumer electronic segment (today representing >80 percent of the total demand) is expected to shrink to less than 10 percent of the total. The compound annual growth rate (CAGR) is estimated at a staggering 33 percent (Figure 4).

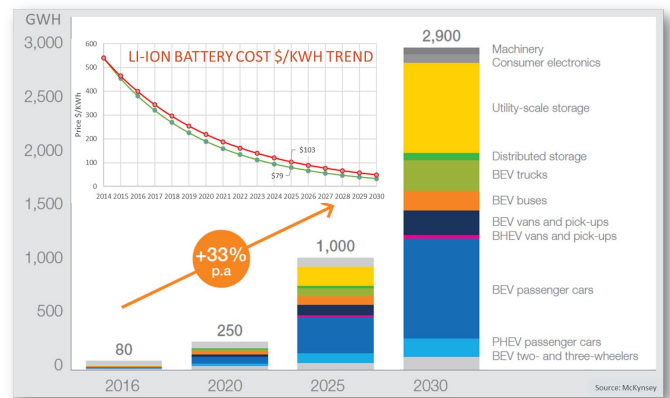


Figure 4: Annual Li-ion battery demand in GWh and cost trend in USD

# The State of The Art

For the last 30 years, industry efforts to advance AC/DC, DC/DC, DC/AC power converter efficiency have been focused on developing: faster switching devices with lower conduction losses (SiC, GaN, Super Junction); further improving the FOM (figure of merit) of IGBT technology; or developing new switching topologies based on legacy Hard-Switching architectures. It should be no surprise then that IGBTs are still the de-facto standard in 99 percent of all inverter designs. It should be expected, however, that the use of SiC and GaN will increase over time as those materials and designs continue their march down the cost curve.

Today, engineers can select from myriad IGBT and MOSFET technologies to develop custom solutions for a wide variety of applications. For instance, several process technologies have been developed to manufacture IGBTs (Figure 5), each of which can be selectively optimized for specific inverter topologies.

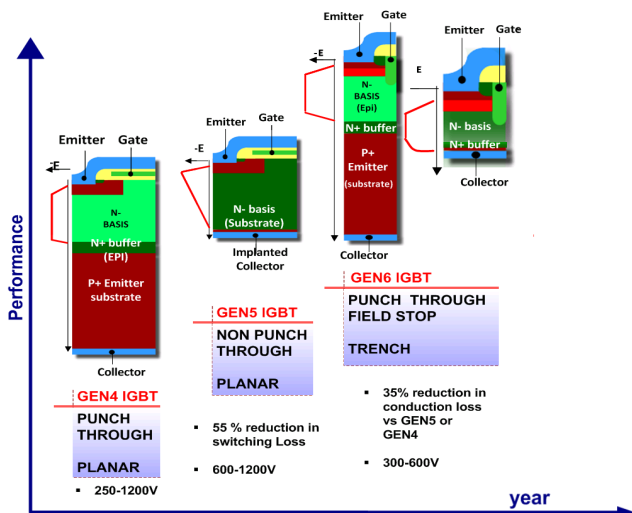


Figure 5: IGBT technology evolution

Field-stop (FS) trench technology, with various adaptations and specializations made by each of the key manufactures, is the bed-rock of inverter designs requiring higher power density and rugged operation. Trench FS IGBTs offer significant improvement in terms of loss

reduction. Most of the newest generation of IGBTs from the major manufactures use combinations of trench cell geometry and field stop structure to enable an optimized carrier concentration. By using this structure, designers increase the carrier density near the trench gate, which yields products with substantially reduced  $V_{CESAT}$ . Additionally, by adopting specific implant and anneal techniques it is possible to deliver low carrier lifetime in proximity of the backside p-emitter that, when combined with a reduced doping and optimized design, allows fast carrier extraction at turn-off with minimized current tail, and therefore obvious benefits for high switching frequency operations.

Further process and design improvements for the trench structure, back side anneal and further thinning of the wafer, are expected to incrementally improve overall energy efficiency in application by reducing power losses. This is the extent of the path available for the incremental improvement for the specific FOM for the IGBTs ( $E_{OFF} \times V_{CESAT}$ ). However, the material limits and additional implementation costs for newer and more sophisticated manufacturing processes still represent a challenging barrier to the optimum improvement of system efficiency with traditional components. On the other hand, all topologies based on Silicon have intrinsically limited improvement capabilities. GaN- or SiC-

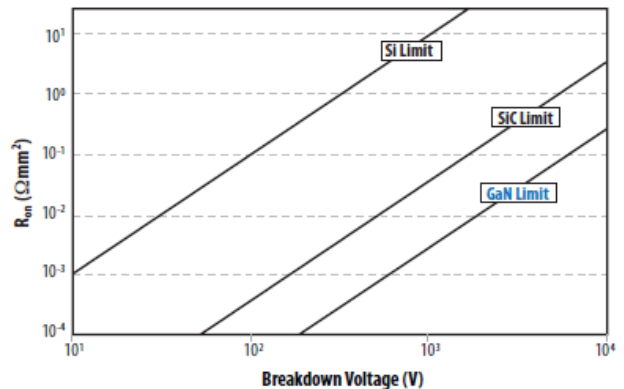


Figure 6: Si-SiC-GaN FOM ( $R_{ONXA}$ ) comparison

## White Paper: The Era of Forced Resonant Soft-Switching

based switches have a better potential FOM than other power components based on Si material (Figure 6). The potential improvement exploitable from the GaN technology is large, based on the material limits [4].

For the inverter stage, in which IGBTs are the standard today, the improvement of FOM:  $V_{CE\text{SAT}} \times E_{TS}$  (Conduction Voltage drop multiplied by Total Switching Energy) provided by GaN based switches, as well as SiC MOSFETs, is almost 3 times lower at a nominal current density of  $2\text{A}/\text{mm}^2$  (Figure 7)

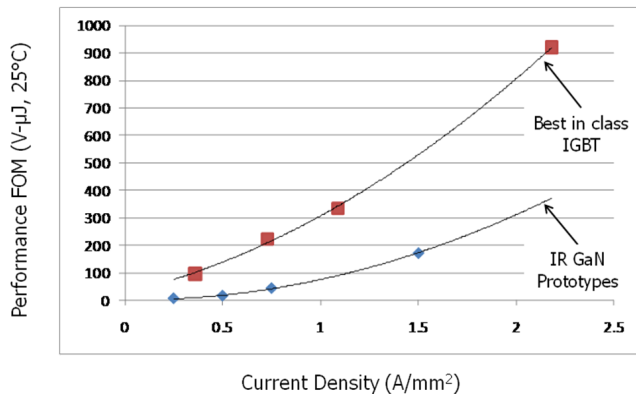


Figure 7: FOM  $V_{CE\text{SAT}} \times E_{TS}$  IGBT vs. GaN

The quest for improvement of the power conversion efficiency—for high-voltage applications in particular—will eventually require the use of advanced semiconductors based on III-V material, like GaN and SiC, not Silicon. The path to further optimize the overall conversion efficiency, for all traditional power conversion topologies, requires a power switch with the lowest possible specific  $R_{ON} \times Q_G$  FOM. The immediate impact of increased operating frequency would have tangible effect on the solar inverter market, for example, with what could be a drastic reduction of the output inductor size, weight, and cost (direct and indirect relative to the overall size of the inverter, installation costs, etc.) The impact of higher frequency operation on output inductor size for a 5KW solar inverter, for example, is significant (Figure 8).

Alas, there is a limit to these improvements since any frequency increase comes with the need to contain the resulting noise and excessive voltage transients. These issues can only be resolved by employing snubbers or by reducing transistor switching speeds. In other words, the practicality of large-scale deployment of new power switches (not to mention the benefits of incremental reduction in power converter size and cost) remain out of reach if power converter operation remains tied to traditional switching architectures.

Silicon, and now III-V-based devices, have steadily improved over time, but they still have not addressed the fundamental limitations of hard-switched architectures. This is the proverbial 800-pound gorilla of the power electronics industry. The limitations of hard-switching keep power converter cost, size, and weight high, while efficiencies remain lower than theoretically possible.

This raises the question: is soft-switching the answer? Even though the concept dates back to the 1980's, soft-switching is still only used in self-resonant DC/DC power converters, which represent only a small fraction of the \$100B+ power converter market today. Soft-switching isolated AC/DC power converters has never been perfected, which is why power engineers call soft-switching for high power AC/DC the 'holy grail' of power electronics.

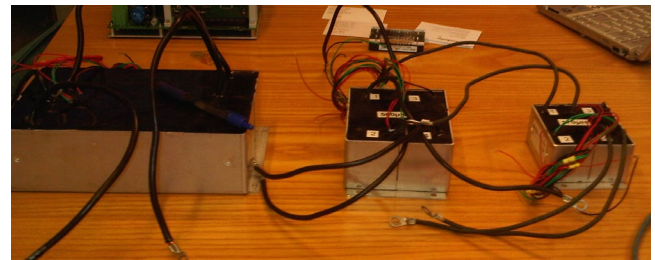


Figure 8: Output inductor comparison of 5KW solar inverters: 20 kHz, 48 kHz, 100 kHz (credit: Fraunhofer Institute)

# A New Path: Soft-Switching with Artificial Intelligence

Pre-Switch, Inc, a Silicon Valley company, has developed a way to resolve the challenges that have kept the industry from making the transition from hard-switching to soft-switching. The Pre-Switch topology for soft-switching is a variation of the Auxiliary Resonant Commutated Pole (ARCP) soft-switching converter topology [11], [12].

Using a sophisticated, embedded Artificial Intelligence (AI), Pre-Switch dynamically solves complex timing calculations to ensure accurate soft-switching under changing input voltage, output load, device tolerances, and temperature changes. These adaptations are made on a cycle-by-cycle basis and work on all soft-switched topologies, including ARCP [13].

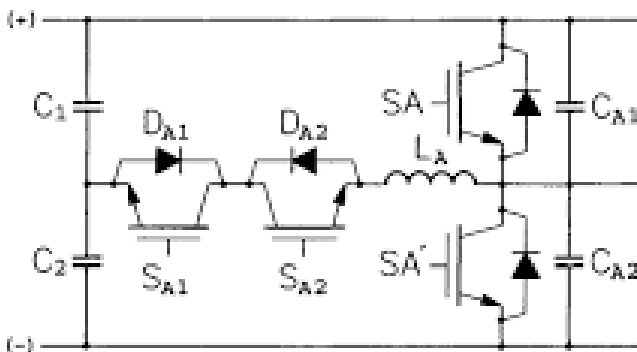


Figure 9: Auxiliary Resonant Commutated Pole Converter (ARCP) schematic

At its most basic, ARCP is a conventional inverter topology with an auxiliary circuit that helps soft-switch the main inverter (Figure 9). The auxiliary switches are activated before the main power output switches are and generate a current in the auxiliary inductor that is used to induce the condition required to soft-switch the main inverter switches. The auxiliary switches are turned on and off at zero current while the main switches are switched at zero voltage.

The innovation developed by Pre-Switch completely resolves the limitations of ARCP soft-switching and enables the reduction or

elimination of switching losses of any power switch. The control algorithm can drive any type of power switch and is ideally suited for anything from silicon-based IGBTs and MOSFETs, to GaN or SiC power switches. The Pre-Switch topology achieves total inverter efficiency with industry standard IGBTs and MOSFETs that is equal to or higher than state-of-the-art III-V material-based power components (SiC & GaN).

Pre-Switch published extensive comparison tests to prove the power loss reductions. These comparisons were performed using standard IGBT power modules; the Infineon EconoDUAL™ FF225R12ME4. The IGBT was tested using a standard double-pulse setup at various temperature and current load conditions. A comparison was made driving the power module with a standard hard-switching gate driver board and then compared to the same power module under the same operating conditions driven by the Pre-Drive gate driver board with the added ARCP network controlled by the Pre-Flex IC. (Figure 10). The additional test circuitry components used were:

- $V_{BUS} = 800V$
- Gate resistors:  $R_{ON}=3.3\text{ohm}$   $R_{OFF}=2.2\text{ohm}$
- Pre-Switch ARCP network: 124nF, 600nH
- Rogowski coil AC Current Probe, Ultra-Mini, 5mV/A, 1200A Peak, 3.2Hz-30MHz (CWT UM/6/B/1/80)

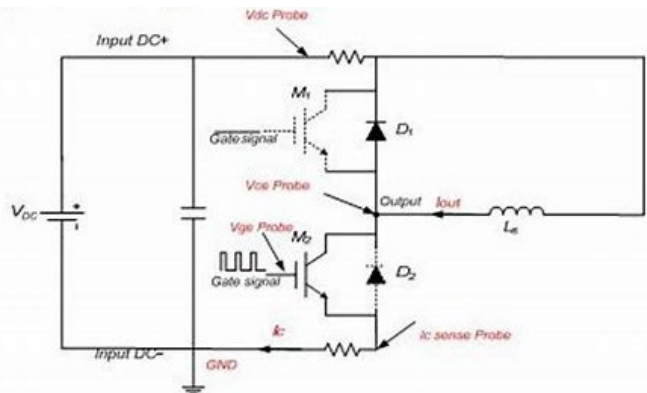


Figure 10: Simplified double-pulse test setup

## Test Results

The results collected during the tests in the laboratory illustrate the dramatic improvement across all key parameters affecting the inverter design, efficiency and noise. The data can be found in Table 1, Table 2, and in the 'Diode  $I_{REC}$  comparison' on the 'Waveform: Turn-On @200A –  $T_C=125^\circ\text{C}$ ' on following pages. Switching energy data, as well as a column labelled 'X-Factor,' can be found in Table 3. The X-Factor is a normalized coefficient that provides the multiplier of the nominal current of the hard-switched inverter stage at the same PWM frequency, that returns the same total power loss, assuming the inverter is operated in soft-switching with the Pre-Switch control algorithm. This factor is a clear indication of the massive

improvement possible when using this soft-switching technique, either in increased current rating of the power stage, or in increased switching frequency (all for the same overall thermal budget of the system). It is also worth noting that using the Pre-Switch soft-switching topology and control algorithm, a regular B6 inverter topology can be used to replace a more complex multilevel configuration, and still offer more total efficiency (not to mention the simplification of the gate driver circuitry).

**(Double pulse test data on following pages)**

Table 1: Commutation  $dV/dt$  @  $T_C = 25^\circ\text{C}$

| IL  | Hard-Switching       | Hard-Switching        | Pre-Switch           | Pre-Switch            |
|-----|----------------------|-----------------------|----------------------|-----------------------|
| A   | Turn-On $dV/dT$ V/ns | Turn-Off $dV/dT$ V/ns | Turn-On $dV/dT$ V/ns | Turn-Off $dV/dT$ V/ns |
| 50  | 4.1                  | 3.9                   | 1.1                  | 0.3                   |
| 200 | 2.2                  | 7.0                   | 1.0                  | 1.2                   |

Table 2: Commutation  $dV/dt$  @  $T_C = 125^\circ\text{C}$

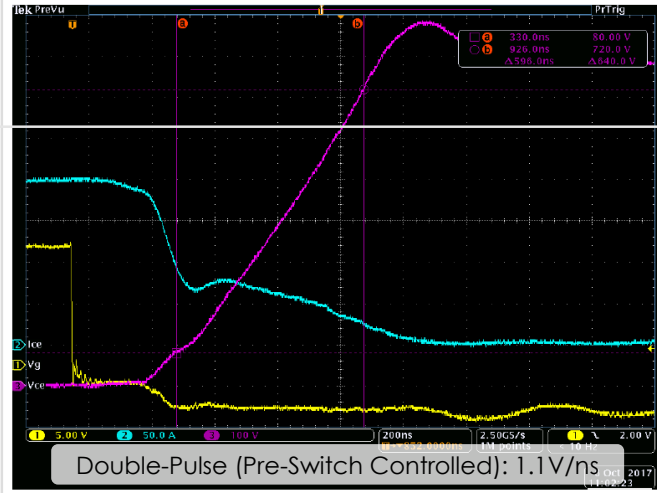
| IL  | Hard-Switching       | Hard-Switching        | Pre-Switch           | Pre-Switch            |
|-----|----------------------|-----------------------|----------------------|-----------------------|
| A   | Turn-On $dV/dT$ V/ns | Turn-Off $dV/dT$ V/ns | Turn-On $dV/dT$ V/ns | Turn-Off $dV/dT$ V/ns |
| 50  | 3.2                  | 2.6                   | 1.1                  | 0.3                   |
| 200 | 1.7                  | 4.2                   | 1.1                  | 1.1                   |

Table 3: Double Pulse Switching Measurement  $E_{ON} - E_{OFF} - E_{REC}$  @  $T_C = 125^\circ\text{C}$

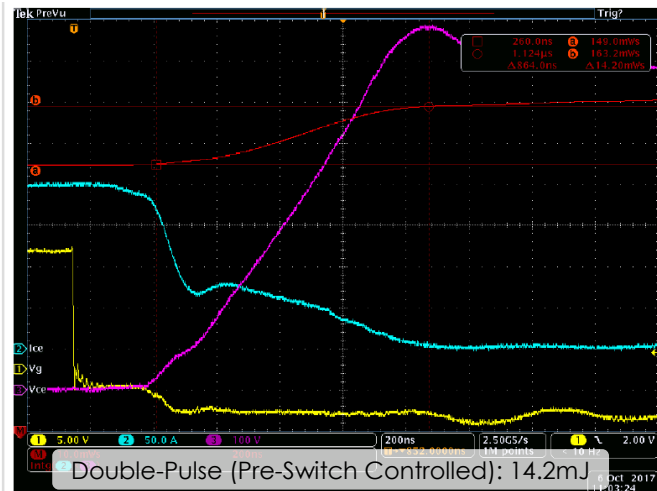
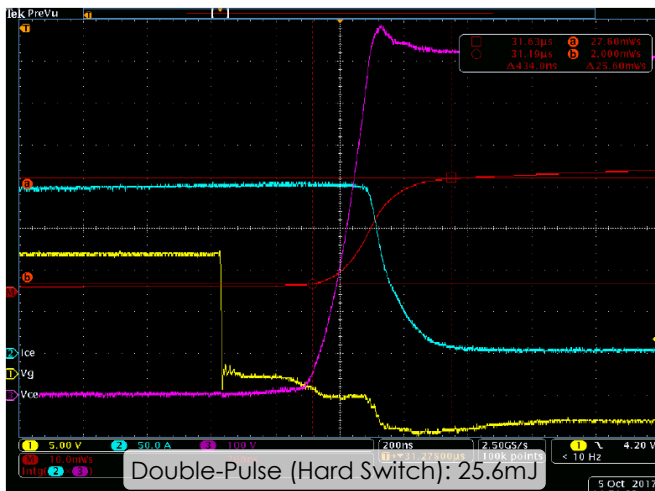
| IL  | Hard-Switching |           |           |           | Pre-Switch Controlled |           |           |           | X Factor | $\Delta$ |
|-----|----------------|-----------|-----------|-----------|-----------------------|-----------|-----------|-----------|----------|----------|
|     | $E_{ON}$       | $E_{OFF}$ | $E_{REC}$ | $E_{TOT}$ | $E_{ON}$              | $E_{OFF}$ | $E_{REC}$ | $E_{TOT}$ |          |          |
| A   | mJ             | mJ        | mJ        | mJ        | mJ                    | mJ        | mJ        | mJ        |          | %        |
| 50  | 14             | 7.8       | 7.8       | 29.6      | 0.4                   | 2.8       | 5.2       | 8.4       | 3.52     | -71.6    |
| 200 | 51.2           | 25.6      | 15.8      | 92.6      | 2                     | 14.2      | 9.8       | 26        | 3.56     | -72      |

# White Paper: The Era of Forced Resonant Soft-Switching

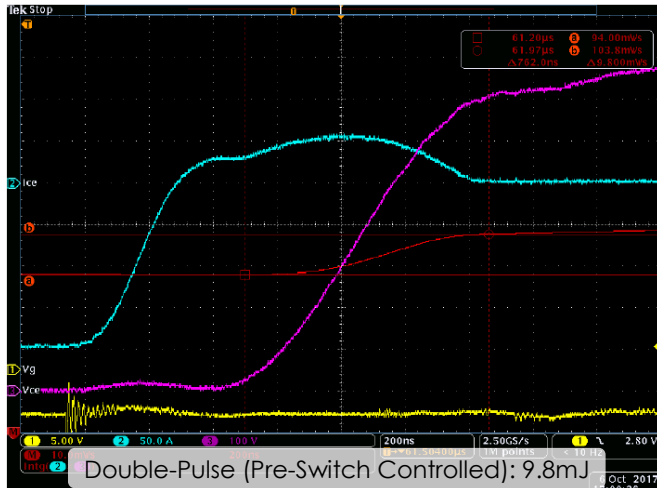
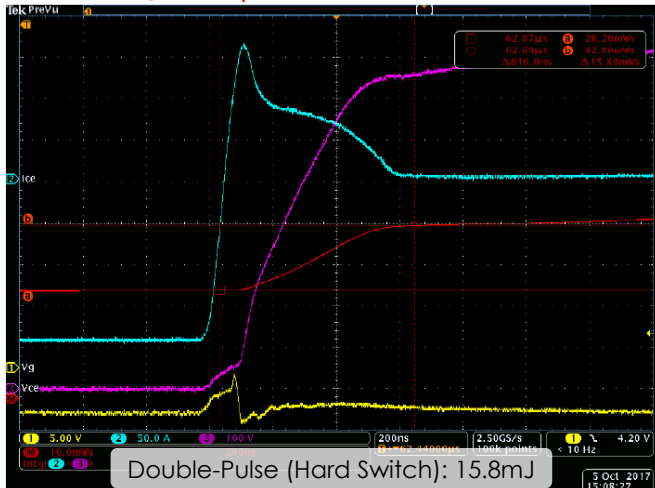
Waveform: Turn-Off @200A –  $T_C = 125^\circ\text{C}$   
dV/dt comparison:



E<sub>OFF</sub> comparison:



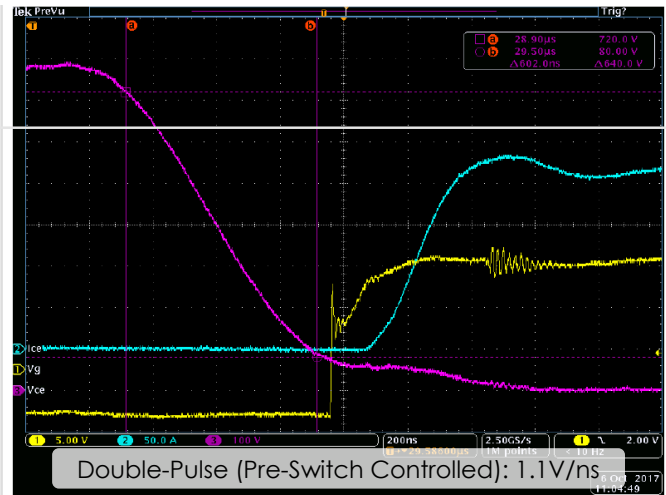
Diode I<sub>REC</sub> comparison:



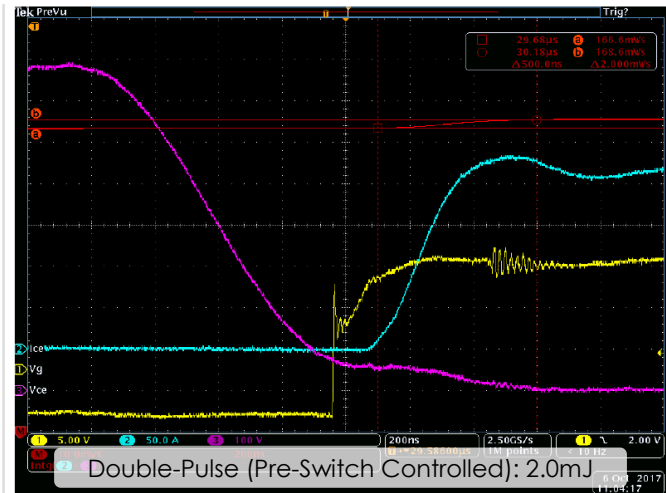
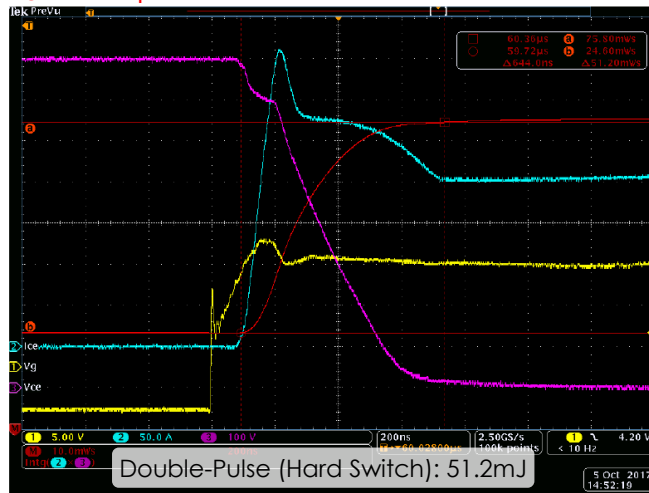
# White Paper: The Era of Forced Resonant Soft-Switching

Waveform: Turn-On @200A –  $T_C = 125^\circ\text{C}$

$dV/dt$  comparison:



$E_{ON}$  comparison:



Diode  $I_{REC}$  comparison:



# Notes on Performance

To correctly consider the net gain in efficiency between the hard-switched condition and the soft-switched condition, the losses added by the control hardware (as per the simplified test setup in Figure 11, required to implement the Pre-Switch control board), the total losses in the auxiliary switches A1 and A2, and the parasitic losses in the resonant network must be considered in the overall efficiency calculation.

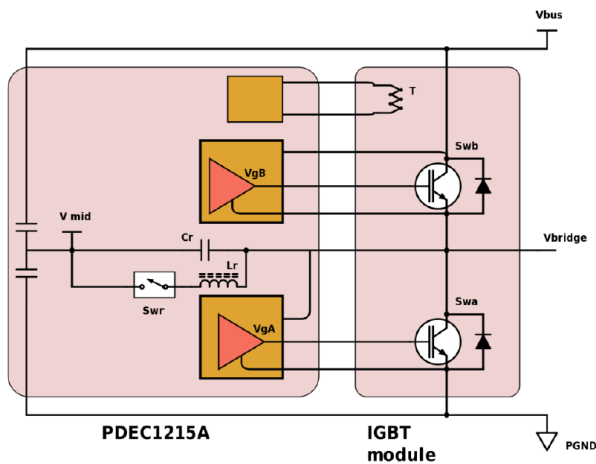


Figure 11: Simplified test setup with Pre-Switch PDCE1215 board

Calorimetric tests (Figure 12) and the modelled auxiliary switching losses are well matched, and

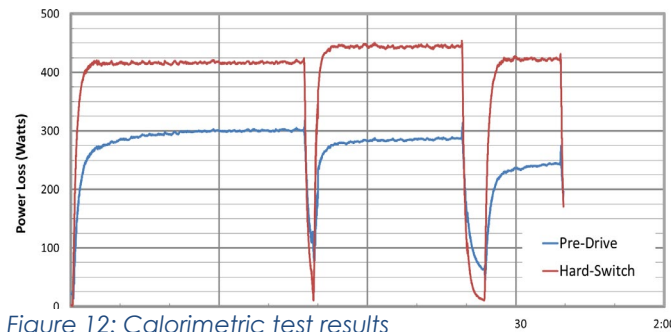


Figure 12: Calorimetric test results

are estimated to be under 20W @200A, 800V, 5kHz. The additional control board, which is operated at 15V line, draws under 2W of total power. The total of 22W is only a fraction of the total efficiency improvement (the switching loss improvement at 200A operation amounts to ~300W). The calorimetric measurement was developed over nearly two hours of full-power testing. In the calorimetric comparison, all power losses (switching, conduction, parasitic, auxiliary) are involved and hence inclusive of the additional auxiliary circuitries of the Pre-Switch topology.

The total power losses and the saving at different test conditions as illustrated in Figure 12 can be found in Table 4. Up to 42% of total power loss reduction has been achieved at the highest frequency of operation. When considering the maximum nominal current of operation allowable in hard-switch mode, the saving with the Pre-Switch, Inc's topology was measured up ~28%.

Table 4: Power losses and savings

| $V_{BUS} = 800V_{DC}$ $R_G = 3.3\Omega$ |        | Pre-Drive      | Hard Switch | $\Delta$ | Saving |
|---|--------|----------------|-------------|----------|--------|
| $I_L$                                   | PWM    | Power Loss [W] |             | [W]      | %      |
| 200A                                    | 5kHz   | 301            | 417         | 116      | 27.8%  |
| 175A                                    | 7.5kHz | 286            | 444         | 158      | 35.6%  |
| 140A                                    | 10kHz  | 243            | 421         | 179      | 42.4%  |

These results are a quantum leap improvement when compared to any other technique known in the power management world. Moreover, the results were obtained without the use of wide band-gap semiconductor materials (III-V group). The gains are attainable with the same IGBT power module and inverter drive. Using the data collected, it is possible to extrapolate an interesting view of how Pre-Switch technology can extend the improvement its topology offers.

# Conclusion

The Pre-Switch topology and control algorithm can deliver wide-bandgap performance with IGBT prices. The overall envelope for the power losses reduction can be modulated, according to the different point of operation in any given type of application, from doubling of current rating and an up to 5x increase in switching frequency operation (Figure 13).

Compared to traditional topologies, Pre-Flex has demonstrated a dramatic reduction in switching losses (70-95%), reduced EMI, and reduced dV/dt. The technology enables low-cost IGBTs to compete favorably with more expensive technologies like SiC MOSFETs and enable SiC technologies to switch up to 20 times faster than they do today, all while solving the dV/dt and EMI problems generated as byproduct of the hard-switching architectures.

The Pre-Switch AI unlocks soft-switching benefits for any power conversion architecture: AC/DC, DC/AC, AC/AC, and DC/DC, isolated, and non-isolated.

**Key facts and demonstrated performance figures**

- Switching loss reduction of 70-95%
  - 1200V IGBT EconoDUAL half bridge power modules double-pulse @125 C tests show a 71% to 82% reduction in switching losses, allowing switching speed increase of 4-5x for the same switching losses
  - 1200V SiC MOSFETs can be switched 15-20x faster for the same switching losses and up to 1 MHz
  - SiC DC/AC inverters have been built with 500KHz to 1 MHz switching frequencies
  - IGBT DC/AC inverters switching at 100KHz
- Increased switching frequencies with reduced dV/dt on IGBT, SiC and GaN, and Super Junction Si
- Power densities higher than 128W/In<sup>3</sup> (7.8W/cm<sup>3</sup>)
- 650V IGBTs are switched at 100kHz
- Cycle-by-cycle control of each transistor enables a new level of reliability and safety

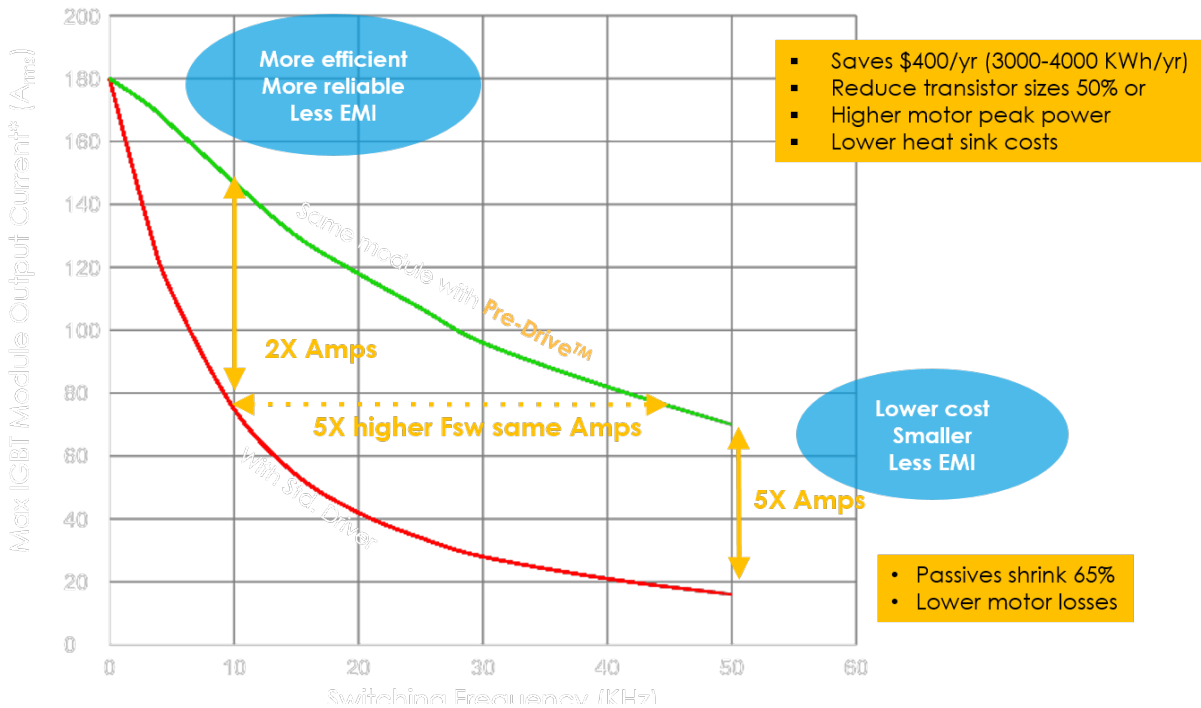


Figure 13: Normalized Total Output Current vs. PWM switching frequency comparison between Hard-Switching operation and Pre-Switch Soft-switching mode

## References & Links

- [1] DOE <http://www.energy.gov/>
- [2] European Community <http://www.intertek.com/electrical/erp-directive/>
- [3] Ebm-papst Magazine 02-2010
- [4] N. Ikeda et.al. ISPSD 2008 p.289
- [5] "(GaN)-based power device technology and its impact on future Efficient Solar grid connected micro-inverters, power optimizers and string inverters". Alberto Guerra and Jason Zhang. PCIM 2010
- [6] "MHz PFC Study and New Architecture ", Chuanyun Wang, Ming Xu CPES 2007
- [7] N.Ikeda et.al. ISPSD 2008 p.289
- [8] Global Solar Demand Monitor published by GTM Research <https://www.greentechmedia.com>
- [9] IHS Markit
- [10] Experimental Investigation of the Performance of Two New Types of Soft-Switching Power Converters for Electric Ships
- [11] De Doncker, R.W.; Lyons, J.P.; "The auxiliary resonant commutated pole converter," Industry Applications Society Annual Meeting, 1990., Conference Record of the 1990 IEEE, vol., no., pp.1228-1235 vol.2, 7-12 Oct. 1990 De Doncker, R.W.; Lyons, J.P.; "The auxiliary resonant commutated pole converter," Industry Applications Society Annual Meeting, 1990., Conference Record of the 1990 IEEE, vol., no., pp.1228-1235 vol.2, 7-12 Oct. 1990
- [12] Resonant system controller and cycle-by-cycle predictive soft switching US 20170179814 A1
- [13] [https://www.mouser.com/datasheet/2/196/infineon\\_FF200R12MT4-1168511.pdf](https://www.mouser.com/datasheet/2/196/infineon_FF200R12MT4-1168511.pdf)